引用格式：ZHANG Chen, HOU Jiaqing, LIN Jiaqi, et al. Investigation on Fabricating Continuous Gradient Micro/nano Needle Structure by Single Femtosecond Laser Voxel (Invited)[J]. Acta Photonica Sinica, 2022, 51(10):1014001
张琛,侯嘉庆,蔺家琪,等. 飞秒激光单体素加工连续渐变微纳针形结构研究(特邀)[J].光子学报,2022,51(10):1014001
※封面论文※

飞秒激光单体素加工连续渐变微纳针形结构研究（特邀）

张琛[1],侯嘉庆[1],蔺家琪[1],李凯[1],范连斌[2],张策[1],王凯歌[1],白晋涛[1]
(1 西北大学 物理学院 光子学与光子技术研究所 省部共建西部能源光子技术国家重点实验室,西安 710127)
(2 中核四〇四有限公司,甘肃 嘉峪关 735100)

摘　要：针对目前微纳针形结构加工中存在的精度、形貌、可控性等问题,基于飞秒激光双光子加工系统中的单个体素,通过引入一维倾角自动调控体素的空间位置,提出了一种简单高效的加工连续渐变微纳针形结构的方法。通过开展加工实验,成功地在光刻胶材料中加工出了一系列长度可控、形貌连续渐变的微纳针形结构。实验结果表明:基于本方法加工的微纳针形结构,其高度呈线性变化关系且针尖形貌渐变精度达到了纳米量级,结构横向线宽渐变连续且沿中轴线呈对称分布;针形结构顶端最小高度达到5 nm,横向最小线宽为195 nm。其在功能表面、微纳流控、生物传感等研究领域具有潜在的应用价值。

关键词：飞秒激光;单体素;双光子聚合;连续渐变;微纳针形结构
中图分类号：O437　　**文献标识码**：A　　**doi**：10.3788/gzxb20225110.1014001

0　引言

形貌连续渐变的微纳针形结构能够产生非对称拉普拉斯压力[1-2]、构建皮牛量级力学环境[3-4]、调节离子迁徙速率[5-6]等,在微液滴操控[7-10]、生物传感[11-14]、离子整流[15-17]等方面有着广泛的应用。

通常,人们利用径迹刻蚀法[18-21]、微球辅助刻蚀[22-24]、微纳米压印[25-27]等技术来加工连续渐变的微纳针形结构。然而,直接通过化学刻蚀方法所获得的微纳针形结构其形貌、变化梯度主要取决于化学试剂对于材料的刻蚀速度、材料膜层的厚度,难以主动地调节结构形貌参数;而微纳米压印技术中所使用的压印模板往往需要电子束曝光结合化学刻蚀等工艺来制备,增加了微纳针形结构的加工成本及加工周期。

近年来,非接触、无掩模的激光直写加工技术发展迅速,为加工微纳针形结构提供了许多新思路。VENTON B J课题组采用双光子聚合(Two-Photon Polymerization,TPP)技术在金属导线端面加工出了聚合物针尖,随后经过碳化处理得到了尖端直径约260 nm的用于体内神经传质检测的针形碳电极[28]。ZAHRA F R等利用TPP技术加工了能够进行药物投递的微针,其为顶部高150 μm、底部直径150 μm,尖端直径约400 nm的微纳针形结构[29]。GU M研究小组基于TPP技术结合精确的平台扫描,加工了长6 μm,底部直径2.4 μm,尖端直径约800 nm的针形结构,可用于仿生应用研究[30]。CHEN F课题组利用材料对飞秒激光脉冲的非线性吸收,在硅玻璃中通过Z轴扫描获得了狭长的改性区域,随后通过湿法刻蚀和倒模得到了高度150 μm,底部半径100 μm,尖端尺寸约2 μm的微米针形结构[31]。此外,MOHAMEED A S等利用KrF

基金项目：国家重大科研仪器研制项目(No. 51927804),国家自然科学基金(Nos. 61378083,61405159, 11504294),国家自然科学基金重大基础研究计划培育项目(No. 91123030),陕西省科技创新团队项目(No. S2018-ZC-TD-0061)
第一作者：张琛(1984—),男,副研究员,博士,主要研究方向为激光技术与应用。Email: nwuzchen@nwu.edu.cn
共同第一作者：侯嘉庆(1996—),男,硕士研究生,主要研究方向为激光微纳米加工技术。Email: houjq@stumail.nwu.edu.cn
通讯作者：王凯歌(1970—),男,研究员,博士,主要研究方向为功能纳米结构研制、纳米生物光子。Email: wangkg@nwu.edu.cn
白晋涛(1959—),男,教授,博士,主要研究方向为激光技术及器件、瞬态光学、激光与物质相互作用。Email: baijt@nwu.edu.cn
收稿日期：2022-07-19;**录用日期**：2022-09-16

准分子激光烧蚀非晶硅，直接获得了尖端直径约10 nm，高度2.5 μm的随机结晶硅纳米尖针形结构阵列[32]；类似地，TAN B等利用飞秒激光烧蚀玻璃，直接制备了相似特征尺寸的簇状纳米尖针阵列[33]。KIANI A等则利用飞秒激光辅助在氮气环境下照射钠钙玻璃表面，通过介质界面附近的等离子体与光脉冲的相互作用获得了高度为2～5 μm，尖端小于100 nm的自由排布的微纳针形结构[34]。

然而，在目前的TPP及激光非线性吸收加工微纳针形结构的过程中，主要通过激光焦点的逐点、逐层扫描来构建结构，针形结构底面直径或高度通常为数微米至百微米级别，尖端加工精度普遍为百纳米量级，不利于构建具有纳米量级连续渐变的针形结构；另一方面，基于激光烧蚀和激光辅助加工的微纳针形结构底面直径以及结构高度通常为数微米，尖端直径可以达到100 nm以下，但是针形结构的形貌和分布具有很大的随机性。针对以上问题，本文提出一种基于飞秒激光双光子系统中的单个体素结合一维倾角控制体素空间位置的加工方法，能够简单高效地加工出具有纳米量级渐变精度的微纳针形结构。随后，实验研究了飞秒激光TPP加工系统体素随功率的变化，并基于不同功率可控加工出了一系列形貌连续渐变的微纳针形结构。通过扫描电镜与原子力显微镜表征与分析，印证了基于本方法加工的微纳针形结构具有结构形貌连续渐变的特征，在高度方向上呈线性变化且达到纳米量级的渐变精度。

1 实验方法

在飞秒激光TPP加工系统中，激光经显微物镜汇聚到样品中与之作用。利用德拜矢量衍射积分公式[35]，模拟数值孔径NA为1.25的物镜对高斯平面波的汇聚（圆偏振，光束充满入瞳），焦平面处光场分布如图1(a)，激光焦点在空间中呈椭球形（入射光波长为λ）。在基于TPP的加工过程中，光聚合反应过程仅发生在激光焦点处，由单个焦点曝光形成的椭球结构，是TPP加工中的基本单元，可将这个特征结构称为Voxel-“体素”。图1(b)为基于本文所使用的飞秒TPP加工系统在入瞳功率为4 mW、曝光时间为50 ms条件下对负性光刻胶加工所获得的体素形貌，其形貌与模拟分布一致，为规则的椭球形（图中比例尺为500 nm）。需要注意的是，加工系统的体素尺寸取决于激光功率、曝光时间、光学系统参数、光刻胶性质等多种因素的共同作用[36-38]，不同加工系统及加工参数下的体素尺寸往往不同。

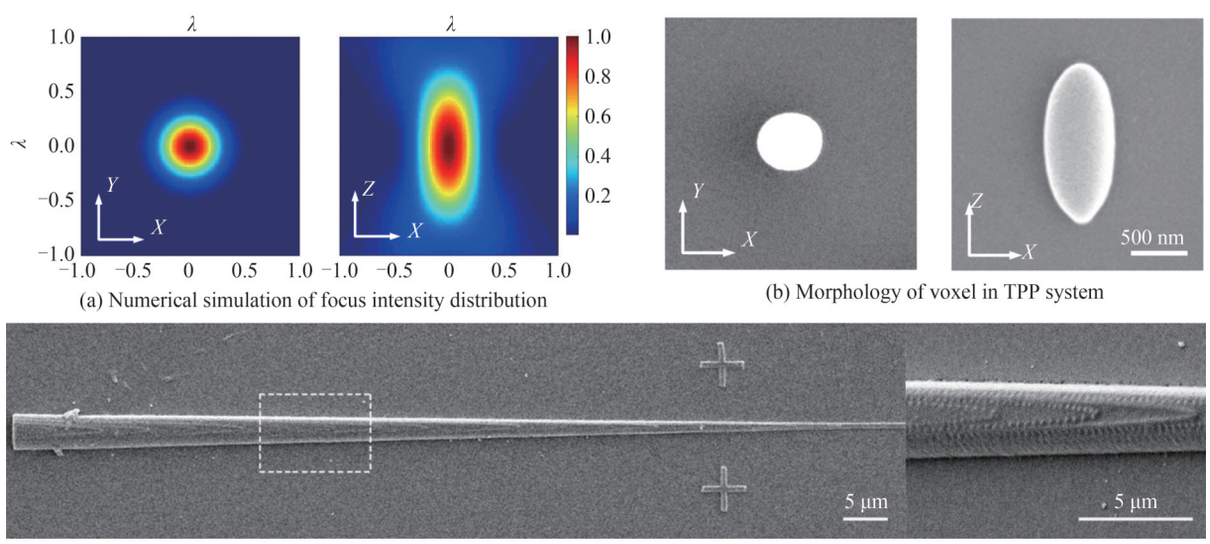

(a) Numerical simulation of focus intensity distribution

(b) Morphology of voxel in TPP system

(c) The morphologic discontinuity of micro/nano needle structure in TPP layer-by-layer scanning

图1 飞秒激光双光子加工体素与层扫描加工微纳针形结构形貌

Fig. 1 The voxel in TPP system and the morphology of micro/nano needle structure utilizing layer-by-layer scanning

在常规的微纳针形结构TPP加工中，通常采用的是逐层扫描的方式，即以单个体素扫描方式勾勒单层结构，最后多层面叠加形成立体结构。图1(c)为使用本文飞秒激光TPP加工系统在功率为3 mW、扫描速度为10 μm/s、扫描间隔200 nm的条件下加工得到的微纳针形结构（图中比例尺为5 μm）。从局部放大图中可知，逐层扫描方式加工的微纳针形结构表面形貌呈现出阶梯结构，而非连续渐变的结构，这必将对后续的实际应用造成不利影响。要减少阶梯结构，则需要利用尺寸更小的体素，同时实施更加精细的分层，这将增

加加工难度和加工时长。

为了获得高精度连续渐变微纳针形结构，提出以体素为基本单元，在激光焦点水平扫描的同时控制其在样品中的轴向空间位置，使其逐步完全沉入基底材料中，即可利用单个体素实现形貌连续渐变的微纳针形结构加工。实际上，如果采取控制水平纳米平台缓慢上升来调控焦点在样品中的轴向空间位置，在加工过程中需要设置运动平台在横向以及轴向的扫描速度进行精准配合，增加了加工过程中的干扰因素。因此，在加工系统中为样品引入一维倾角，以实现焦点在轴向的高精度自动调节。其原理如图2(a)，加工初始时刻为样品引入一个一维倾角α，随后控制平台沿X轴水平运动，激光焦点将自动的沉入样品基底中，从而在光刻胶中加工出形貌渐变的微纳针形结构。

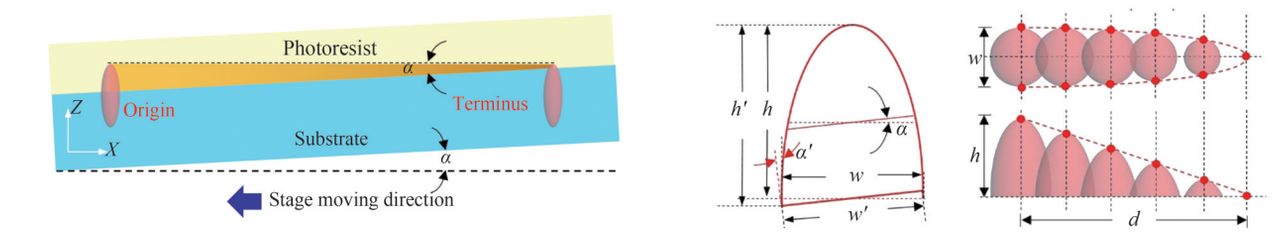

(a) Implementation of needle structure by introducing one-dimensional angle　(b) Structural analysis

图2　单体素加工原理及结构分析

Fig. 2　Schematic of fabricating needle structure with single voxel and structural analysis

由图2(b)可知，引入一维角度调控后实际体素的横向线宽$w'=2w/\cos\alpha+w\tan\alpha\cdot\tan\alpha'$，体素高度$h'=h+\tan\alpha\cdot w/2$。由于本方法中引入的一维倾角非常小，倾角的引入对于体素横向线宽以及高度的影响可以忽略。基于此方法得到的微纳针形结构，理论上，其横向线宽将逐步由体素横向线宽w收缩至0 nm，其轴向线宽将由轴向线宽h线性的降至0 nm；结构与体素加工的轴向半高h、倾角α与结构长度d之间关系为$d=h/\tan\alpha$。

2　实验装置

图3(a)为飞秒TPP加工系统光路示意图，系统使用800 nm、150 fs、80 MHz重复频率的飞秒激光作为激发光源(Coherent，Chameleon Ultra Ⅱ)，使用半波片和格兰棱镜组合以及衰减片调控激光功率，机械光闸Shutter(Thorlabs，SC10)控制激光光束通断。飞秒激光经过二色镜Dichroic Mirror反射进入NA=1.25，100倍率显微镜物镜Objective(Olympus，Apoplan)聚焦至样品中。样品台的运动由压电陶瓷纳米平台Nano Stage

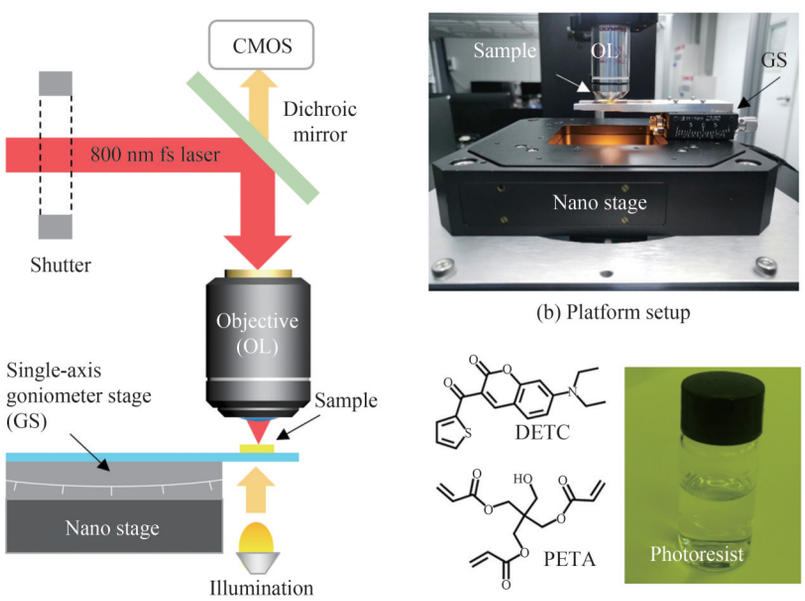

(a) Schematic diagram of TPP system　(b) Platform setup　(c) Photoresist

图3　实验装置及样品成分

Fig. 3　Experimental setup and sample composition

(PI, P-562.6CD)控制,单轴倾斜摆台 Single-axis Goniometer Stage(OptoSigma, GOHT-40A75)为样品引入一维倾角。加工过程中利用安全光对样品进行明场照明,实时图像经物镜与二向色镜后由 CMOS 相机(大恒光电,MER-2000-19U3C-L)采集,图 3(b)为系统加工平台装置实拍。

实验选用适合用于双光子聚合加工的光引发剂 7-二乙氨基-3-噻吩甲酰基香豆素(7-Diethylamino-3-thenoylcoumarin, DETC)(Exciton,1176692),将其溶于季戊四醇三丙烯酸酯(Pentaerythritol triacrylate, PETA)(Sigma-Aldrich)单体,质量分数为 0.5 wt%。PETA 是一种交联程度很高的负性光刻胶单体,聚合后具有较高的机械强度,避免结构在显影过程中被破坏,DETC 与 PETA 化学式如图 3(c)所示。此外,PETA 中还添加有 300 ppm~400 ppm(1 ppm=0.000 1%)的单甲基醚对苯二酚(Monomethyl ether hydroquinone)(Sigma-Aldrich)抑制剂,能增加光刻胶的保存时间,并在一定程度上抑制双光子聚合过程来提高分辨率[39]。制备光刻胶时在室温将两者按照 0.5∶100 的比例充分混合,将单体引发剂混合物置于磁力搅拌器搅拌约 24 h,获得颜色均一的透明状液体后静置备用。

3 实验结果与分析

飞秒激光双光子加工系统的体素尺寸是由激光功率、曝光时间、扫描速度以及光刻胶性质等共同决定的,不同组合的加工参数下的体素尺寸有可能相似。在实际应用中只需要标定体素的大小,随后可以设计相应的针形结构的加工参数。为了方便对加工结果的分析,设定实验中扫描速度、光刻胶材料的配比不变,首先选取入瞳处激光功率作为变量,通过不同的功率参数实现不同尺寸微纳针形结构加工。

设置入瞳处激光功率分别为 3、4、5、6、7 mW,曝光时间为 50 ms,可得相应的 TPP 加工体素如图 4(a)所示。体素的横向线宽分别为 294、478、542、621、668 nm,轴向线宽分别为 720、1 151、1 561、1 841、2 060 nm,体素横向、轴向线宽的增长速率随着功率的增加逐渐降低。

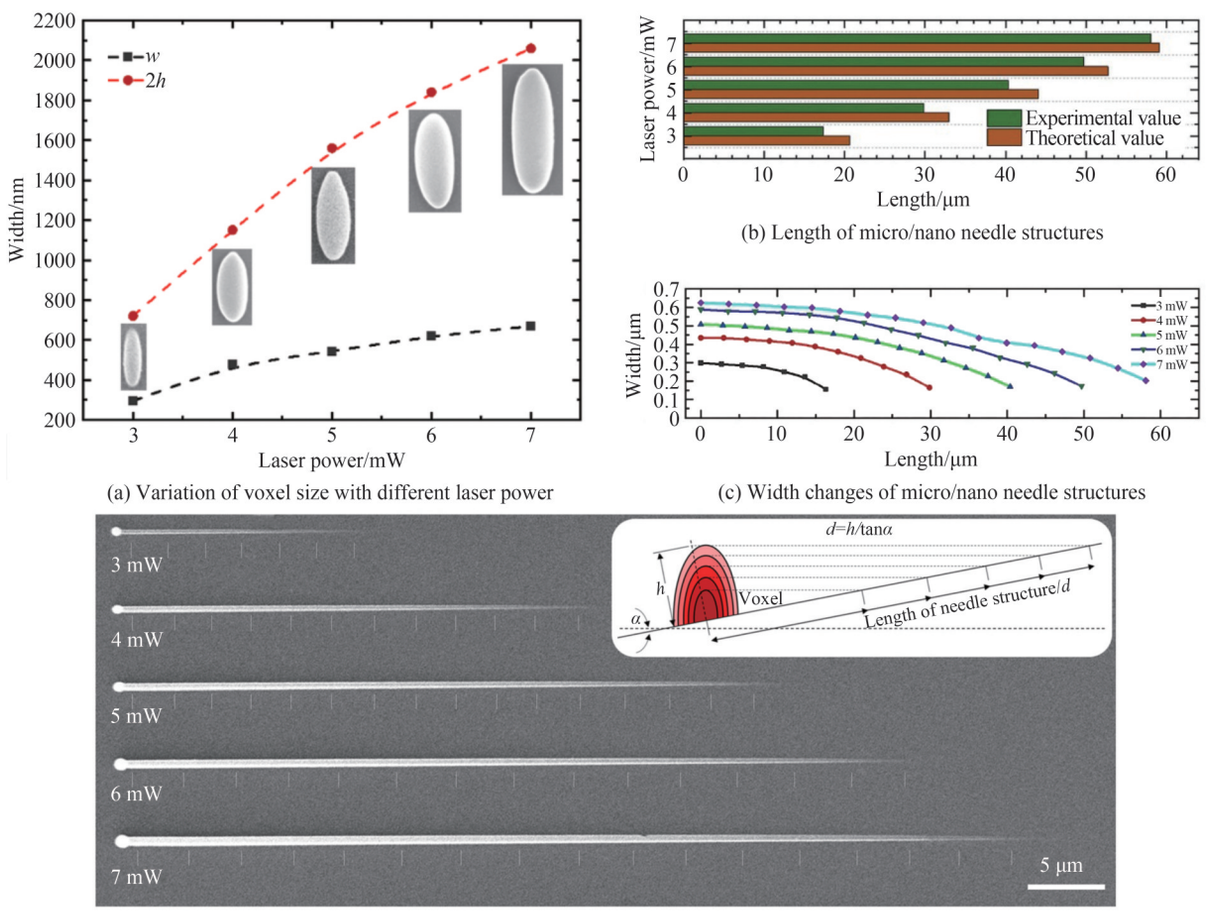

(a) Variation of voxel size with different laser power

(b) Length of micro/nano needle structures

(c) Width changes of micro/nano needle structures

(d) SEM image of micro/nano needle structure fabricated by different laser power

图 4 微纳针形结构加工实验结果及分析

Fig. 4 Experimental results and analysis of micro/nano needle structures

设置一维摆台倾角为1°，加工起始时刻激光焦点中心位于基片表面。设置入瞳处激光功率分别为3、4、5、6、7 mW。取体素的横向线宽与曝光时间的比值w/t作为与上述所得体素结构的曝光时间对应的行进速度（w取值500 nm）。纳米平台行进速度恒定为10 μm/s，加工微纳针形结构时平台沿X轴负方向运动。其加工结果的扫描电镜SEM影像如图4(d)（图中比例尺为5 μm），在不同的加工功率获得的长度不同，线宽渐变减小的微纳针形结构。由4(b)可知，在当前实验条件下，实验加工结构长度分别为17.3、29.8、40.4、49.7、58.1 μm，略小于理论上的结构长度。其主要原因可能是：当焦点逐步沉入基底时，引发游离基生成的有效光强减小造成游离基浓度降低，从而削减了体素尺寸，进而使加工结构长度小于理论长度。结构横向线宽的总体变化趋势如图4(c)，由曲线可知，在结构的前半段，尺度变化较为平缓，而后半段的线宽变化较快，这是由单体素的结构特征所决定的。但这并不影响整体结构的变化连续性，不存在图1(c)中的形貌变化不连续的情况。

为进一步获取微纳针形结构的尖端部分的形貌，在此选择3 mW、7 mW的尖端结构（长度8 μm），利用原子力显微镜（Atomic Force Microscope，AFM）分别进行表征，从结构尖端处起，每隔750 nm取一个位点（取样长度6 μm），共取9个位点做截面轮廓扫描。图5(a)为3 mW飞秒激光单体素加工结果，沿其中轴线（图中虚线所示）以及“1、2、3、4、5、6、7、8、9”九个位点作轮廓扫描。九个位点处的结构中轴高度分别为94、83、72、59、45、29、19、11、5 nm，在沿中轴线方向上，针尖结构的高度在表征区域内呈现出纳米量级连续线性变化，结构倾角为0.96°；九个位点处的结构半高宽分别为480、450、435、405、375、350、320、290、195 nm，从截面轮廓图可知结构的形貌相对于中线左右宽度相当，结构整体呈现均匀的对称分布。图5(b)为7 mW飞秒激光单体素加工结果，通过对中轴线以及九个位点作轮廓扫描，其结构高度分别为140、124、105、89、64、43、28、15、7 nm，针尖结构的高度在沿中轴线方向上同样呈现出连续线性变化，结构倾角为1.05°；结构半高宽分别为510、490、475、455、410、385、355、330、230 nm，结构形貌同样是均匀对称分布。

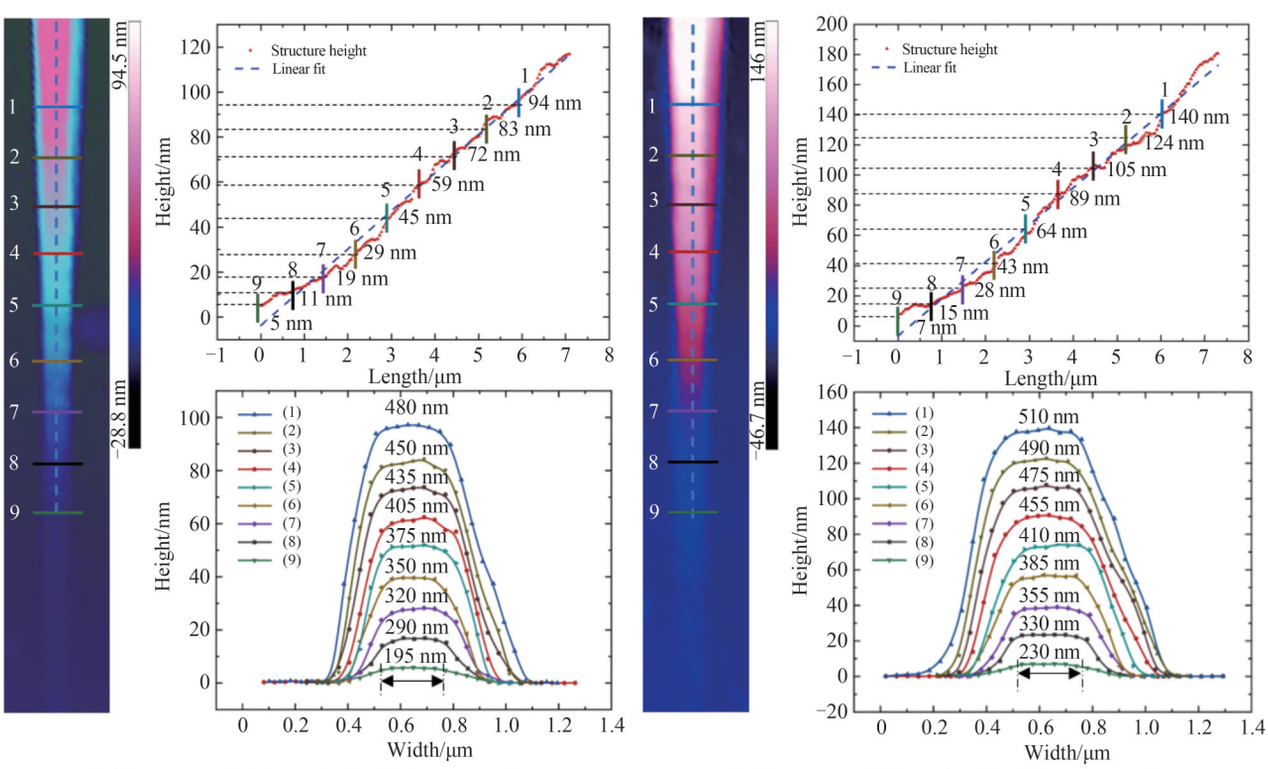

(a) Tip structure fabricated by 3 mW femtosecond laser　　(b) Tip structure fabricated by 7 mW femtosecond laser

图5　针尖结构AFM影像及其形貌分析

Fig. 5　AFM image and morphology analysis of the tip structure

由AFM扫描结果可知，基于本方法得到了尖端远小于体素尺寸的针形结构，且垂直方向上加工的精度达到了10 nm以内，这是传统激光加工方式无法实现的。但同时，由于受到光学系统衍射极限的限制，体素顶端较为平坦，因此微纳针形结构尖端的横向加工精度低于垂直方向加工精度。

样品的倾斜角度也会对微纳针形结构的长度和形貌产生影响。如图6(a)所示，倾角α与结构长度d之间存在关系$d=h/\tan\alpha$，改变倾角α时，体素沉入基底所需的距离也会发生改变，随之改变了结构长度d。设置入瞳处激光功率为4 mW，设置α分别为1°、1.5°、2°、2.5°，扫描速度及光刻胶的参数与前文实验一致，其加工结果的扫描电镜SEM影像如图6(c)(图中比例尺为3 μm)。当α分别为2.5°、2°、1.5°、1°时，结构长度d分别为12.3、17.1、21.5、32.4 μm，结构的长度随倾角的减小而增加；微纳针形结构形貌变化速率与α成正相关。图6(b)展示了在当前实验条件下，不同倾角下所得结构的实际长度和理论长度的对比图，实验与理论预期高度一致，表明了本方法同样可以通过调节倾角来实现微纳针形结构的可控加工。需要注意的是，由于样品角度的转动点与激光焦点位置不同，在调整样品角度时加工位置就会发生改变，所以在同一结构的加工过程中不能通过实时改变角度来调节结构形貌。

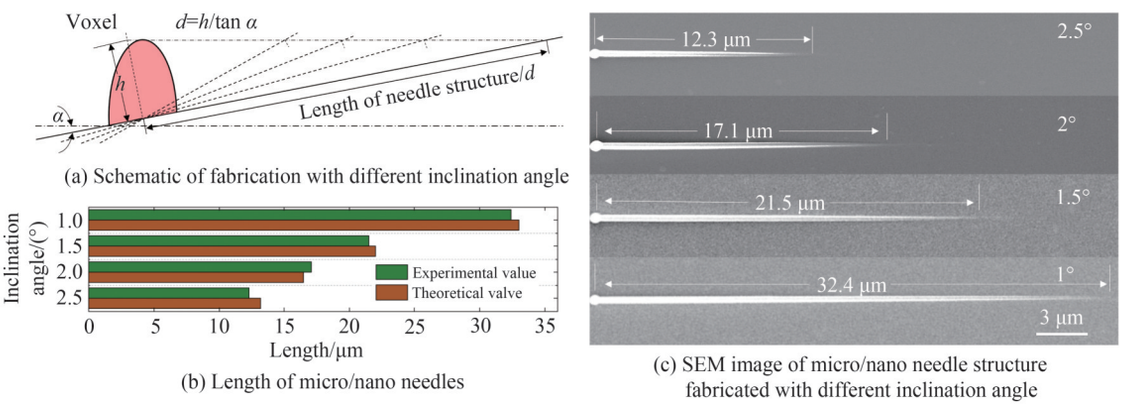

图6 微纳针形结构加工实验结果及分析

Fig. 6 Experimental results and analysis of micro/nano needle structures

综上，基于本方法可以可控地加工不同长度和渐变速率的微纳针形结构，且所得的微纳针形结构形貌连续渐变，实验结果与理论预测具有很高的一致性。从AFM扫描结果可知，受益于本方法的加工原理，微纳针形结构在高度方面呈现出线性度很高的渐变，其渐变误差在数个纳米的量级，最小高度可达到5 nm；而宽度的渐变则是关联于体素的形状特征，初始阶段渐变较为缓慢，随着加工的进行，渐变逐步加快，最小尖端宽度为195 nm。但整体而言，结构形貌的渐变都是一个平滑的渐变过程，其不存在阶梯状的渐变趋势。同时，值得注意的是，通过调试激光功率、曝光时间、光刻胶等实验参数能够进一步降低TPP加工体素的尺寸，从而减小微纳针形结构的尖端宽度特征。

4 结论

基于飞秒TPP加工系统的单个体素，成功地在光刻胶中实现了一系列形貌连续渐变的微纳针形结构的加工。在入瞳功率分别为3、4、5、6、7 mW，平台移动速度为10 μm/s，一维倾角为1°的条件下，结构长度分别达到17.3、29.8、40.4、49.7、58.1 μm，符合理论预期值。通过原子力显微镜对3、7 mW功率下加工的针尖结构进行表征，其高度呈现出连续线性变化，且精度达到纳米量级；结构倾角分别为0.96°与1.05°，与一维倾角契合。此外，在倾角分别为1°、1.5°、2°、2.5°，入瞳功率为4 mW而其它参数不变的条件下，加工了相应的微纳针形结构，所获得的结构长度与理论值相吻合，结构形貌变化率与倾角正相关。另一方面，微纳针形结构的横向线宽关联于体素的形状特征，在针尖处呈现较快的渐变，但始终为平滑连续渐变，不存在阶梯状的跳变。在本研究中，加工获得的微纳针形结构顶端最小高度达到5 nm，横向最小线宽为195 nm，在微纳流体力学、微流控、生物大分子检测、仿生核孔等研究方面具有潜在的应用价值。

参考文献

[1] CUI Z, XIAO L, LI Y, et al. A fishbone-inspired liquid splitter enables directional droplet transportation and spontaneous separation[J]. Journal of Materials Chemistry A, 2021, 9(15): 9719-9728.

[2] LI Y, CUI Z, LI G, et al. Directional and adaptive oil self-transport on a multi-bioinspired grooved conical spine[J]. Advanced Functional Materials, 2022, 32(27): 1035-1045.

[3] DAI L, DOYLE P S. Comparisons of a polymer in confinement versus applied force[J]. Macromolecules, 2013, 46(15):

6336-6344.
[4] BONTHUIS D J, MEYER C, STEIN D, et al. Conformation and dynamics of DNA confined in slitlike nanofluidic channels[J]. Physical Review Letters, 2008, 101(10): 108303.
[5] SIWY Z. Ion-current rectification in nanopores and nanotubes with broken symmetry[J]. Advanced Functional Materials, 2006, 16(6): 735-746.
[6] PATRICIO R, PAVEL Y A, JAVIER C, et al. Pore structure and function of synthetic nanopores with fixed charges: tip shape and rectification properties[J]. Nanotechnology, 2008, 19(31): 315707.
[7] ZHENG Y, BAI H, HUANG Z, et al. Directional water collection on wetted spider silk[J]. Nature, 2010, 463(7281): 640-643.
[8] JU J, BAI H, ZHENG Y, et al. A multi-structural and multi-functional integrated fog collection system in cactus[J]. Nature Communications, 2012, 3(1): 1247-1253.
[9] CHEN H, ZHANG P, ZHANG L, et al. Continuous directional water transport on the peristome surface of nepenthes alata[J]. Nature, 2015, 532(7597): 85-89.
[10] WANG Y, ZHANG M, LAI Y, et al. Advanced colloidal lithography: from patterning to applications[J]. Nano Today, 2018, 22(1): 36-61.
[11] LIU M, ZHANG H, LI K, et al. A bio-inspired potassium and pH responsive double-gated nanochannel[J]. Advanced Functional Materials, 2014, 25(3): 421-426.
[12] LIU Q, XIAO K, WEN L, et al. Engineered ionic gates for ion conduction based on sodium and potassium activated nanochannels[J]. Journal of the American Chemical Society, 2015, 137(37): 11976-11983.
[13] WU K, XIAO K, CHEN L, et al. Biomimetic voltage-gated ultra-sensitive potassium-activated nanofluidic based on solid-state nanochannel[J]. Langmuir the Acs Journal of Surfaces & Colloids, 2017, 33(34): 8463-8467.
[14] ZHAO X, WANG S, XIA X, et al. Asymmetric nanochannel-ionchannel hybrid for ultrasensitive and label-free detection of copper ions in blood[J]. Analytical Chemistry, 2018, 90(1): 896-902.
[15] YMILI T, VANINA C, GREGORIO L, et al. Ion track-based nanofluidic biosensors[J]. Miniaturized Biosensing Devices, 2022, 5(7): 57-81.
[16] WANG J, ZHOU Y, JIANG L. Bio-inspired track-etched polymeric nanochannels: steady-state biosensors for detection of analytes[J]. ACS Nano, 2021, 15(12): 18974-19013.
[17] WU J, WANG S, LIANG Y, et al. Investigation on the competition of duplex/g-quadruplex/i-motif in telomere sequences and c-myc gene with a solid-state nanopore sensor[J]. Sensors and Actuators B Chemical, 2021, 348(1): 130712.
[18] XIA F, GUO W, MAO Y, et al. Gating of single synthetic nanopores by proton-driven DNA molecular motors[J]. Journal of the American Chemical Society, 2008, 130(26): 8345-8395.
[19] MARIA E, TOIMIL M. Characterization and properties of micro-and nanowires of controlled size, composition, and geometry fabricated by electrodeposition and ion-track technology[J]. Beilstein J Nanotechnol, 2012, 3(97): 860-883.
[20] NIU B, XIAO K, HUANG X, et al. High-sensitivity detection of iron (Ⅲ) by dopamine-modified funnel-shaped nanochannels[J]. ACS Applied Materials & Interfaces, 2018, 10(26): 22632-22639.
[21] SUN Y, CHEN S, CHEN X, et al. A highly selective and recyclable NO-responsive nanochannel based on a spiroring opening-closing reaction strategy[J]. Nature Communications, 2019, 10(1): 1323-1330.
[22] ANDREAS H, CHRISTIAN S, KATHARINA B, et al. Parallel fabrication of plasmonic nanocone sensing arrays[J]. Small, 2013, 9(23): 3987-3992.
[23] LI N, DOU S, FENG L, et al. Enriching analyte molecules on tips of superhydrophobic gold nanocones for trace detection with saldi-ms[J]. Talanta, 2019, 205(1): 120085.
[24] ZHU Q, ZHAO X, ZHANG X, et al. Au nanocone array with 3D hotspots for biomarker chips[J]. CrystEngComm, 2020, 22(31): 5191-5199.
[25] AMALRAJ P, AMALATHAS, MAAN M A. Upright nanopyramid structured cover glass with light harvesting and self-cleaning effects for solar cell applications[J]. Journal of the American Chemical Society, 2016, 49(46): 465601.
[26] SI S, LARS D, MARTIN H. The nanotufe-fabrication of large area periodic nanopatterns with tunable feature sizes at low cost[J]. Microelectronic Engineering, 2017, 180(5): 71-80.
[27] ZHANG W, ZHANG J, WU P, et al. Parallel aligned nickel nanocone arrays for multiband microwave absorption[J]. ACS Applied Materials&Interfaces, 2020, 12(20): 23340-23346.
[28] CAO Q, MIMI S, NICKOLAY V, et al. 3D-printed carbon nanoelectrodes for in vivo neurotransmitter sensing[J]. Nano Letter, 2020, 20(9): 6831-6836.
[29] FARAJI R, NORDON R, ANTHONY C, et al. High-fidelity replication of thermoplastic microneedles with open microfluidic channels[J]. Microsystems & Nanoengineering, 2017, 3(1): 17034.
[30] DING H, ZHANG Q, GU Z, et al. 3D computer-aided nanoprinting for solid-state nanopores[J]. Nanoscale Horizons,

2018, 10(3): 312-316.
[31] BIAN H, YANG Q, CHEN F, et al. Scalable shape-controlled fabrication of curved microstructures using a femtosecond laser wet-etching process[J]. Materials Science and Engineering, 2013, 33(5): 2795-2799.
[32] SARA M, JOUMANA E, MOHAMED A. Swillam one step fabrication of silicon nanocones with wide-angle enhanced light absorption[J]. Scientific Report, 2018, 8(1): 4001-4011.
[33] SAMARASEKERA C, TAN B, VENKATAKRISHNAN K. Ultrafast laser synthesized nanostructures for controlling cell proliferation[J]. J. Biomed. Nanotechnol, 2015, 11(4): 623-630.
[34] AMIRKIANOOSH K, NIKUNJ B P, BO T, et al. Leaf-like nanotips synthesized on femtosecond laser-irradiated dielectric material[J]. Journal of Applied Physics, 2015, 117(7): 074306.
[35] LEUTENEGGER M, RAO R, LEITGEB R A, et al. Fast focus field calculations[J]. Optics Express, 2006, 14(23): 11277-11291.
[36] BOUGDID Y, MAOULI I, RAHMOUNI A, et al. Systematic λ/21 resolution achieved in nanofabrication by two-photon-absorption induced polymerization[J]. Journal of Micromechanics and Microengineering, 2019, 29(3): 035018.
[37] ZHOU X, HOU Y, LIN J, et al. A review on the processing accuracy of two-photon polymerization[J]. AIP Advances, 2015, 5(3): 030701.
[38] SUN H, TAKADA K, KIM M, et al. Scaling laws of voxels in two-photon photopolymerization nanofabrication[J]. Applied Physics Letters, 2003, 83(6): 1104-1106.
[39] FISCHER J, MUELLER J B, KASCHKE J, et al. Tree-dimensional multi-photon direct laser writing with variable repetition rate.[J]. Optics Express, 2013, 21(22): 26244-26260.

Investigation on Fabricating Continuous Gradient Micro/nano Needle Structure by Single Femtosecond Laser Voxel (Invited)

ZHANG Chen[1], HOU Jiaqing[1], LIN Jiaqi[1], LI Kai[1], FAN Lianbin[2],
ZHANG Ce[1], WANG Kaige[1], BAI Jintao[1]
(1 *State Key Laboratory of Photon-technology in Western China Energy, Institute of Photonics & Photon Technology, School of Physics, Northwest University, Xi'an* 710127, *China*)
(2 *The* 404 *Company Limited China National Nuclear Corporation, Jiayuguan, Gansu* 735100, *China*)

Abstract: Micro-nano needle structure with continuously gradient morphology has the capacity of generating asymmetric Laplace pressure, simulating mechanical environment in nano newton grade, adjusting the ion migration rate etc., therefore, it has been widely applied in many fields such as microdroplet manipulation, biosensors, and ion rectification. However, in the previous fabrication of micro-nano needle structures with Two-Photon Polymerization (TPP), the structures were mainly constructed through the layer-by-layer scanning of laser focus. The bottom diameter or the height of the needle structure was usually in the grade of several or hundreds of micrometers. Further, the processing accuracy of the needles was generally in the grade of 100 nm, which resulted in the discontinuous morphology of the needle structures. On the other hand, the bottom diameter and structure height of micro-nano needle structures based on laser ablation or laser-assisted processing could be several micrometers, and the tip diameter could be less than 100 nm, however, the morphology and distribution of the needle structures were highly random. Considering the problems of precision, morphology and controllability in the previous fabrication of micro-nano needle structures, this paper proposes a novel method utilizing single voxel of femtosecond laser two-photon system to creating micro-nano needle-shaped structure with continuously changing morphology. In this methodology, a one-dimensional inclination angle is brought in the platform to automatically and linearly adjust the laser voxel to axially sink into the substrate completely as the stage is horizontally scanning. Finally, a micro-nano needle structure with continuous gradient morphology is produced. It is well known that, the voxel size in two-photon processing is the joint action of laser power, exposure time, scanning speed, and photoresist properties etc., the voxel might have similar size with different processing parameter combinations. Therefore, in this methodology, the size of the voxel should be calibrated firstly, and then people can determine the incline angle and corresponding processing parameters for the fabrication of needle-shaped structures. In order to facilitate the analysis of

the processing results, in this investigation the scanning speed and the composition of photoresist materials are constant, and the laser power at the entrance pupil or inclination angle is selected as the variable to prepare micro-nano needle structures with different sizes. The TTP system in the experiment is built up based on femtosecond laser with a center wavelength of 800 nm. The photoresist is prepared with DETC as the initiator and PETA as the monomer. A single-axis goniometer stage, which is mounted on high precision nano stage, is utilized to configure the inclination angle of the sample. In the calibration, the laser power at entrance pupil is tuned to 3, 4, 5, 6, and 7 mW to produce the voxels with 50 ms exposure time. The lateral width of the corresponding voxels are 294, 478, 542, 621, 668 nm respectively. Meanwhile, the axial width of these voxels are respectively 720, 1 151, 1 561, 1 841, 2 060 nm. The increasing rate of lateral and axial line width will decline with the increase of power. Then, in the micro-nano needle structure fabrication, the center of the laser focus is located on the surface of the substrate at the beginning of fabrication. The incline angle is set to 1° and the platform scanning speed is 10 μm/s for scanning. A series of micro-nano needle structures with controllable length and gradually changing morphology are fabricated with fore-mentioned laser configurations. The SEM images show that the micro-nano needle structures with length of 17.3, 29.8, 40.4, 49.7, 58.1 μm are successfully obtained based on this method, which are slightly shorter than the theoretical fabrication length. It is probably caused by the declined in the concentration of the radical. As the focus gradually sink into the substrate, the effective laser intensity for exciting free radicals will decrease and lower the concentration of free radicals. Therefore, the voxel size will be reduced and result in a shorter length of micro-nano needle structure. At the same time, when the laser power is 4 mW, the inclination angles are 1°, 1.5°, 2°, and 2.5°, and other parameters are constant, the experiment fabricated structure length is consistent with the theoretical calculation. On the other hand, the topographic change gradient is positively correlated with inclination angle. It is also found that, the lateral line width of the micro-nano needle-shaped structure changes gently at the beginning of the fabrication, and changes quicker near as approaching to the end. This variation trend is determined by the structural characteristics of the single voxel, however, it does not affect the change continuity of the overall structure. The morphology change of the micro-nano needle in lateral direction is continuous in SEM observation. Further, it is seen from the AFM scanning results that benefiting from the processing principle of this fabrication methodology, the micro-nano needle structure exhibits a high-linearly gradient in height. The gradient fluctuation of the nano tips is in the order of several nanometers, and the minimum height of the nano tips could reach 5 nm. By using AFM calibration, the morphology of the nano tips are exhibited. The lateral line width gradient of the tip structure is smooth, and there are no step-like jump points. The minimum line width of the nano tips reaches 195 nm. It is noticed that, the nano tip structure changes faster in axial direction than lateral direction due to the shape feature of the voxel. In conclusion, the methodology that proposed in this work is effective and convenient for fabricating the micro-nano needle structures with high accuracy. The morphology of the experimentally fabricated needle structures are continuously gradated, and the precision of the fabrication achieved at the nanometer level. In addition, the experimental results are in high consistent with the theoretical predictions. It is worthy to mention that, the size of the TPP processing voxel can be further optimized by adjusting factors such as laser power, exposure time, photoresist, etc., which could produce finer and sharper nano tip structures. Such structures have potential applications in functional surfaces, micro-nano fluidics, and biosensing and other research fields.

Key words: Femtosecond laser; Single voxel; Two-photon polymerization; Continuous gradient; Micro/nano needle structure

OCIS Codes: 140.3390; 190.4710; 220.3740; 220.4241

Foundation item: National Major Scientific Research Instrument Development Project of China (No. 51927804), National Natural Science Foundation of China (Nos. 61378083, 61405159, 11504294), Major Basic Research Program of the National Natural Science Foundation of China (No. 91123030), Science and Technology Innovation Team Project of Shaanxi Province (No. S2018-ZC-TD-0061)